MATCH
Communications in Mathematical and in Computer Chemistry

MATCH Commun. Math. Comput. Chem. **95** (2026) 5–21
ISSN: 0340–6253
doi: 10.46793/match.95-1.03025

The Use of Haar Wavelet Functions for Solving Two Problems in Chemistry

Morteza Bisheh-Niasar*, **Mehdi Sabzevari**

Department of Applied Mathematics, Faculty of Mathematical Sciences, University of Kashan, Kashan, Iran

mbisheh@kashanu.ac.ir, sabzevari@kashanu.ac.ir

(Received February 21, 2025)

Abstract

In this paper, we present a numerical technique to solve two mathematical models corresponding to two problems in the field of chemistry. One of these problems delves into the dynamic interplay of carbon substrates and oxygen concentrations within a microbial floc particle. Another problem relates to the chemical reaction of carbon dioxide CO2 and phenyl glycidyl ether in solution. The proposed method is based on Haar wavelet functions. This method reduces the problems mentioned to sets of algebraic equations. The method is straightforward, and numerical results validate its effectiveness. To demonstrate its efficiency, we have compared the numerical results to some existing results.

1 Introduction

Many chemical processes in mathematical modeling are represented by second-order boundary value problems. It is well-known that most of these problems do not have a closed-form exact solution. In such cases, one possible approach is to use numerical methods. Here, we will mention two

*Corresponding author.

cases of modeling chemistry problems.

• Domestic and industrial wastewater contains a high concentration of destructive carbonaceous organic materials. The primary method for treating organic waste is activated sludge. This biological process effectively oxidizes the carbon substrates, converting them into new cells (sludge), carbon dioxide (CO2), and water (H2O). Excess sludge is the primary byproduct that is expensive to treat and dispose of. Once anaerobic bacteria dominate, the sludge can quickly become putrescent, necessitating its removal from the sedimentation tank before this occurs. The concentrations of carbon substrates and oxygen primarily influence the amount of sludge. Therefore, it is essential to investigate new methods to minimize sludge production.

In [1, 7, 11], a mathematical model was introduced that describes the relationship between the concentration of carbon substrate and oxygen concentration. This model consists of a system of two coupled Lane–Emden-type equations and it is used to model the excess sludge production in wastewater treatment plants and is represented by the following equation:

$$\begin{cases} xu''(x) + 2u'(x) = -\alpha_2 x + xF_1(u(x), v(x)), \\ xv''(x) + 2v'(x) = xF_2(u(x), v(x)), \end{cases} \tag{1}$$

subject to the conditions

$$u'(0) = 0, \; u(1) = 1, \; v'(0) = 0, \; v(1) = 1. \tag{2}$$

In Eq(1), x represents the radius of a spherical floc particle and the functions $u(x)$ and $v(x)$ denote the concentrations of carbon substrate and oxygen, respectively. Furthermore, F_1 and F_2 are defined as

$$F_1(u(x), v(x)) = \frac{\alpha_1 u(x)v(x)}{(l_1 + u(x))(m_1 + v(x))} + \frac{\alpha_3 u(x)v(x)}{(l_2 + u(x))(m_2 + v(x))},$$
$$F_2(u(x), v(x)) = \frac{\alpha_4 u(x)v(x)}{(l_1 + u(x))(m_1 + v(x))} + \frac{\alpha_5 u(x)v(x)}{(l_2 + u(x))(m_2 + v(x))}.$$

For Eq(1), Muthukumar et al. [11] utilized the Adomian decomposition method, while Duan et al. [7] combined the Adomian decomposition method with the Duan-Rach modified recursion scheme. Additionally, In [20], the variational iteration method has also been employed for this problem. Also, Saadatmandi and Fayyaz have solved this BVP using the sinc-collocation method and Chebyshev finite difference method, numerically [13, 14].

• For the chemical kinetics problem of carbon dioxide CO2 and phenyl glycidyl ether(PGE), following [12] we can use a coupled model of nonlinear differential equations for the steady-state concentrations of CO2 and PGE as:

$$\begin{cases} u''(x) = \frac{\alpha_1 u(x)v(x)}{1+\beta_1 u(x)+\beta_2 v(x)}, \\ v''(x) = \frac{\alpha_2 u(x)v(x)}{1+\beta_1 u(x)+\beta_2 v(x)}, \end{cases} \tag{3}$$

$$u(0) = 1, \quad u(1) = k, \quad v'(0) = 0, \quad v(1) = 1. \tag{4}$$

In the above system, $u(x)$ and $v(x)$ represent the dimensionless concentrations of CO2 and PGE, respectively and α_i and β_i (where $i = 1, 2$) are defined constants. The variable x denotes the dimensionless distance measured from the center, and k represents the dimensionless concentration of CO2 at the surface of the catalyst. In [8, 12], the authors employed the Adomian decomposition method to solve the system model and its associated boundary conditions. In [18], an optimal homotopy analysis method was applied, and the authors in [15], utilized the residual method for this problem. Al-Jawari and Radhi [4] applied the variational iteration method to solve the equations (3), with boundary conditions (4). Also, Zabihi has solved these coupled equations numerically by using the Chebyshev finite difference method and Sinc-collocation method [21, 22].

For equations (1,3) and their corresponding boundary conditions, we will apply the Haar wavelet method. In recent years, the Haar wavelet method has gained popularity in the field of numerical approximation due to its advantages and properties. This method is simple to apply and is suitable for both initial value problems (IVPs) and boundary value problems (BVPs) and various conditions can be easily accommodated.

In [19], Tantawy presented an effective approach using the Haar wavelet technique to solve linear systems of fractional integro-differential equations, focusing on the Fredholm and Volterra forms. The authors in [2] applied the Haar wavelet and higher-order Haar wavelet collocation methods to nonlinear ordinary differential equations, considering various initial conditions, boundary conditions, periodic conditions, two-point conditions, integral conditions and multi-point integral boundary conditions. In another study [9], second-order boundary value problems were addressed using Haar wavelets. An efficient and accurate method based on Haar wavelets was developed for solving third and fourth-order differential equations with nonlocal boundary conditions [6]. Additionally, a hybrid numerical method, combining Haar wavelets and finite difference methods, was proposed to solve the hyperbolic telegraph interface model with discontinuous coefficients [5]. The authors in [3] also utilized two numerical methods based on Haar wavelets and higher-order Haar wavelets to solve linear and nonlinear fourth-order differential equations with different types of boundary conditions, including two-point boundary conditions and two-point integral boundary conditions. In [16,17], the Haar wavelet technique has been applied for second and third-order Emden-Fowler types with a variety of initial and boundary conditions.

This paper is organized as follows: In Section 2, we review the basic definitions of Haar wavelet functions and their fundamental properties. Section 3 presents a computational method for solving Problems (1) and (3) using Haar wavelet functions. In Section 4, we provide numerical results to illustrate the efficiency of the proposed method and compare them with existing outcomes. Finally, section 5 is devoted to the conclusion.

2 Haar wavelets

In this section, we define the Haar wavelet family on in the interval $[0, 1)$. For this goal, J is introduced as the maximal of resolution and we define $M = 2^J$. Now we define the Haar wavelet family as

$$H_1(x) = \begin{cases} 1 & 0 \leq x < 1, \\ 0 & otherwise, \end{cases} \tag{5}$$

and for $j = 0, 1, \cdots, J, \quad m = 2^j, \quad \kappa = 0, 1, \cdots, m-1$ and $i = m + k + 1$:

$$H_i(x) = \begin{cases} 1 & \lambda_1 \leq x < \lambda_2, \\ -1 & \lambda_2 \leq x < \lambda_3, \\ 0 & otherwise, \end{cases} \tag{6}$$

where $\lambda_1 = \frac{\kappa}{m}$, $\lambda_2 = \frac{\kappa+0.5}{m}$, $\lambda_3 = \frac{\kappa+1}{m}$. Here, j represents the wavelet resolution level and called as the dilation parameter, while κ denotes the translation parameter. The Haar wavelets family has the following properties:

$$\int_0^1 H_i(x)dx = \begin{cases} 1 & i = 1, \\ 0 & i \neq 1, \end{cases}$$

$$\int_0^1 H_i(x)H_l(x)dx = \begin{cases} 0 & i \neq l, \\ m^{-1} & i = l = m + \kappa + 1. \end{cases}$$

So the functions $H_i(x)$ are orthogonal. For simplicity, we will define the following notation to denote the Haar wavelet integrals:

$$p_{i1}(x) = \int_0^x H_i(t)dt, \quad p_{i2}(x) = \int_0^x p_{i1}(t)dt. \tag{7}$$

These integrals can be evaluated as [16, 17]:

$$p_{11}(x) = x,$$

$$p_{i1}(x) = \begin{cases} x - \lambda_1 & \lambda_1 \leq x < \lambda_2, \\ \lambda_3 - x & \lambda_2 \leq x < \lambda_3, \\ 0 & otherwise, \end{cases} \quad i = 2, 3, \cdots$$

$$p_{12}(x) = \frac{x^2}{2},$$

$$p_{i2}(x) = \begin{cases} \frac{1}{2}(x-\lambda_1)^2 & \lambda_1 \le x < \lambda_2, \\ \frac{1}{4m^2} - \frac{1}{2}(\lambda_3 - x)^2 & \lambda_2 \le x < \lambda_3, \\ \frac{1}{4m^2} & \lambda_3 \le x < 1, \\ 0 & otherwise. \end{cases} \qquad i = 2, 3, \cdots .$$

In recent years, several numerical techniques utilizing Haar wavelets have been proposed to solve differential equations and integro-differential equations. Most of these methods employ Chen and Hsiao's methodology. According to this methodology, the highest-order derivative in the model is approximated using a truncated Haar wavelet series as $\sum_{i=1}^{2M} a_i H_i(x)$.

3 The computational method based on Haar wavelets

In this section, we use Haar wavelet functions to approximate solution of eq(1) and eq(3), corresponding to their stated conditions. For domain [0 1) we define the collocation points as

$$x_t = \frac{t-0.5}{2M}\ , \quad t = 1, 2, \cdots, 2M. \tag{8}$$

3.1 Applying the Haar wavelet technique to the eq. (1)

Using Haar wavelets, the highest order derivative terms in eq(1) can be approximated as

$$u''(x) \approx \sum_{i=1}^{2M} a_i H_i(x), \quad v''(x) \approx \sum_{i=1}^{2M} b_i H_i(x). \tag{9}$$

By integrating the first above equation twice from 0 to x and applying boundary conditions, we have

$$u'(x) - u'(0) \approx \sum_{i=1}^{2M} a_i p_{i1}(x) \to u'(x) \approx \sum_{i=1}^{2M} a_i p_{i1}(x); \tag{10}$$

$$u(x) - u(0) \approx \sum_{i=1}^{2M} a_i p_{i2}(x). \tag{11}$$

Thus

$$u(1) - u(0) \approx \sum_{i=1}^{2M} a_i p_{i2}(1) \to u(0) \approx 1 - \sum_{i=1}^{2M} a_i p_{i2}(1). \tag{12}$$

Therefore, we have

$$u(x) \approx 1 + \sum_{i=1}^{2M} a_i \left(p_{i2}(x) - p_{i2}(1)\right). \tag{13}$$

The similar process can be done for $v(x)$ and its derivatives. Now, by inserting collocation points (8), into eq(1), we obtain the following nonlinear system:

$$\begin{cases} x_t u''(x_t) + 2u'(x_t) = -\alpha_2 x_t + x_t F_1(u(x_t), v(x_t)), \\ x_t v''(x_t) + 2v'(x_t) = x_t F_2(u(x_t), v(x_t)), \quad t = 1, 2, \cdots, 2M \end{cases} \tag{14}$$

where

$$\begin{cases} u''(x_t) \approx \sum_{i=1}^{2M} a_i H_i(x_t), \\ u'(x_t) \approx \sum_{i=1}^{2M} a_i p_{i1}(x_t), \\ u(x_t) \approx 1 + \sum_{i=1}^{2M} a_i \left(p_{i2}(x_t) - p_{i2}(1)\right), \end{cases} \tag{15}$$

$$\begin{cases} v''(x_t) \approx \sum_{i=1}^{2M} b_i H_i(x_t), \\ v'(x_t) \approx \sum_{i=1}^{2M} b_i p_{i1}(x_t), \\ v(x_t) \approx 1 + \sum_{i=1}^{2M} b_i \left(p_{i2}(x_t) - p_{i2}(1)\right). \end{cases} \tag{16}$$

Eqs(14) generate $4M$ non-linear equations which can be solved to obtain the unknown coefficients $a_i, b_i,\ i = 1, \cdots, 2M$.

Theorem 1. *Assume that $u^{(s)}(x),\ v^{(s)}(x), s = 1, 2, 3$ exist and are bounded. If $u_J, v_J(x)$ are the obtained approximate solutions based on Haar wavelet and $u(x), v(x)$ are the exact solutins of eq(1), then as $J \to \infty$, we* *have*

$$\|u(x) - u_J(x)\|_\infty < O(\frac{1}{M^2}), \quad \|v(x) - v_J(x)\|_\infty < O(\frac{1}{M^2}).$$

Proof. $u''(x)$ can be expanded into a Haae series as $u''(x) = \sum_{i=1}^{\infty} a_i H_i(x)$. Similar to mentioned process, By integrating twice and substituting boundary conditions, the exact solution is written in the following form

$$u(x) = 1 + \sum_{i=1}^{\infty} a_i \left(p_{i2}(x) - p_{i2}(1)\right). \tag{17}$$

On other hand

$$u_J(x) = 1 + \sum_{i=1}^{2M} a_i \left(p_{i2}(x) - p_{i2}(1)\right), \tag{18}$$

is the numerical solution obtained at Jth resolution, therefore

$$\begin{aligned} \|E_J\|_\infty \qquad &= \|u(x) - u_J(x)\|_\infty = \| \sum_{i=2M+1}^{\infty} a_i \left(p_{i2}(x) - p_{i2}(1)\right) \|_\infty \\ &= \max_x | \sum_{i=2M+1}^{\infty} a_i \left(p_{i2}(x) - p_{i2}(1)\right) | \rightarrow \end{aligned}$$

$$\|E_J\|_\infty \leq \max_x \sum_{i=2M+1}^{\infty} |a_i| \left(|p_{i2}(x)| + |p_{i2}(1)|\right). \tag{19}$$

From [10], the wavelet coefficients a_i's can be calculated by

$$\begin{aligned} a_i = 2^j \int_0^1 u''(x) H_i(x) dx &= 2^j \left(\int_{\lambda_1}^{\lambda_2} u''(x) dx - \int_{\lambda_2}^{\lambda_3} u''(x) dx \right) \\ = 2^j \left(u''(\xi_1)(\lambda_2 - \lambda_1) - u''(\xi_2)(\lambda_3 - \lambda_2)\right), \end{aligned}$$

where $\xi_1 \in (\lambda_1, \lambda_2), \xi_2(\lambda_2, \lambda_3)$. It is easy to verify that

$$\lambda_2 - \lambda_1 = \lambda_3 - \lambda_2 = \frac{1}{2^{j+1}},$$

thus

$$a_i = \frac{1}{2}\left[u''(\xi_1) - u''(\xi_2)\right] = \frac{1}{2}(\xi_1 - \xi_2)u'''(\xi),\ \xi \in (\xi_1, \xi_2).$$

$u'''(x)$ is bounded, then for positive constant γ, we have

$$|a_i| \leq \frac{\gamma}{2^{j+1}}. \tag{20}$$

In [10], it is demonstrated with details that

$$\max_{x\in(0,1)} p_{i2}(x) = (\frac{1}{2^{j+1}})^2. \tag{21}$$

From eq(20) and eq(21) we have

$$\begin{aligned}\|E_J\|_\infty &\leq 2\gamma \sum_{i=2M+1}^{\infty} \frac{1}{2^{j+1}}\left(\frac{1}{2^{j+1}}\right)^2 = 2\gamma \sum_{j=J+1}^{\infty}\sum_{k=0}^{2^j-1}\left(\frac{1}{2^{j+1}}\right)^3 \\ &= \gamma \sum_{j=J+1}^{\infty}\left(\frac{1}{2^{j+1}}\right)^2 = \frac{\gamma}{3}\left(\frac{1}{2^{J+1}}\right)^2 = O(\frac{1}{M^2}).\end{aligned}$$

The similar result is hold for v. ■

3.2 Applying the Haar wavelet technique to the eq. (3)

Similar to previous subsection, we can approximate $u''(x)$ and $v''(x)$ by using Haar wavelet functions and obtain $u(x)$ and $v(x)$ by integrating repeatedly to find $u(x), u'(x)$, $v(x)$ and $v'(x)$. Same as before, for $v(x)$ we have

$$v''(x) \approx \sum_{i=1}^{2M} b_i H_i(x), \quad v(x) \approx 1 + \sum_{i=1}^{2M} b_i \left(p_{i2}(x) - p_{i2}(1)\right). \tag{22}$$

But for $u(x)$ and its derivatives, by integrating twice from 0 to x, we have

$$u''(x) \approx \sum_{i=1}^{2M} a_i H_i(x) \to u'(x) - u'(0) \approx \sum_{i=1}^{2M} a_i p_{i1}(x); \tag{23}$$

$$(u(x)-u(0))-xu'(0)\approx\sum_{i=1}^{2M}a_ip_{i2}(x). \tag{24}$$

Hence for $x=1$ we have:

$$u'(0)\approx u(1)-u(0)-\sum_{i=1}^{2M}a_ip_{i2}(1).$$

Above equation is substituted in eq(24), therefore

$$u(x)\approx 1+x\left(k-1-\sum_{i=1}^{2M}a_ip_{i2}(1)\right)+\sum_{i=1}^{2M}a_ip_{i2}(x). \tag{25}$$

Now, we insert the collocation points (8) into Eqs(3):

$$\begin{cases}(1+\beta_1u(x_t)+\beta_2v(x_t))u''(x_t)=(\alpha_1u(x_t)v(x_t)),\\ (1+\beta_1u(x_t)+\beta_2v(x_t))v''(x_t)=\alpha_2u(x_t)v(x_t),\end{cases} \tag{26}$$

where

$$\begin{cases}u''(x_t)\approx\sum_{i=1}^{2M}a_iH_i(x_t),\\ u(x_t)\approx 1+x\left(k-1-\sum_{i=1}^{2M}a_ip_{i2}(1)\right)+\sum_{i=1}^{2M}a_ip_{i2}(x_t),\end{cases} \tag{27}$$

$$\begin{cases}v''(x_t)\approx\sum_{i=1}^{2M}b_iH_i(x_t),\\ v(x_t)\approx 1+\sum_{i=1}^{2M}b_i\left(p_{i2}(x_t)-p_{i2}(1)\right).\end{cases} \tag{28}$$

By solving eqs(26), we can easily calculate the coefficients a_i and $b_i,\ i=1,\cdots,2M$. Throughout this paper, we use the Maple's **fsolve** command for solving this non-linear system.
Similar to Theorem 1, we can present a corresponding theorem regarding the convergence order of the Haar wavelet-based technique applied to eq(3), concluding that

$$\|u(x)-u_J(x)\|_\infty<O(\frac{1}{M^2}),\quad \|v(x)-v_J(x)\|_\infty<O(\frac{1}{M^2}).$$

4 Numerical experiments

In this section, we present numerical simulations derived from the proposed technique for solving equations (1) and (3). Throughout this section, $u_J(x)$ and $v_J(x)$ show the approximate solutions obtained for parameter J.

Example 1. For the first problem, consistent with the approach outlined in [13, 14, 20] we set

$$m_1 = m_2 = l_1 = l_2 = 0.0001,$$
$$\alpha_1 = 5,\ \alpha_2 = 1,\ \alpha_3 = \alpha_4 = 0.1,\ \alpha_5 = 0.05.$$

To facilitate comparison, Tables (1) and (2) display the results of the proposed Haar wavelet method(HWM) alongside those obtained using the variational iteration method [20], Sinc-collocation method [13] and classical 4−th order Runge-Kutta method (with a constant stepsize $h = 0.1$).

Table 1. comparison of results of $u_4(x)$, for equation (1).

x	HWM($J=4$)	Sinc-C [13]	VIM [20]	RK
0.1	0.3237600	0.3238492	0.3238516	0.3426228
0.3	0.3786995	0.3784715	0.3784898	0.3960602
0.5	0.4876834	0.4877298	0.4877663	0.5011594
0.7	0.6516180	0.6516395	0.6516811	0.6596803
0.9	0.8702081	0.8702122	0.8702341	0.8727150

Table 2. comparison of results of $v_4(x)$, for equation (1).

x	HWM($J=4$)	Sinc-C [13]	VIM [20]	RK
0.1	0.9752576	0.9752602	0.9752603	0.8441813
0.3	0.9772568	0.9772589	0.9772595	0.8572612
0.5	0.9812553	0.9812567	0.9812578	0.8818643
0.7	0.9872534	0.9872541	0.9872553	0.9189154
0.9	0.9952512	0.9952513	0.9952519	0.9694035

To evaluate the accuracy of our approximate solution, similar to [14,20], we define the error remainder functions

$$ER_{u,J}(x) = xu''_J(x) + 2u'_J(x) + \alpha_2 x - xF_1(u_J(x), v_J(x)),$$

$$ER_{v,J}(x) = xv''_J(x) + 2v'_J(x) - xF_2(u_J(x), v_J(x)),$$

and the maximal error remainder parameters

$$MER_{u,J} = \max_{x\in[0,1)} |ER_{u,J}(x)|, \quad MER_{v,J} = \max_{x\in[0,1)} |ER_{v,J}(x)|. \qquad (29)$$

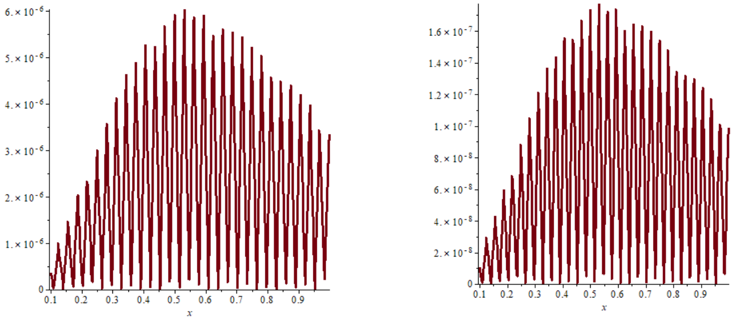

Figure 1. Plot of the $|ER_{u,4}(x)|$ (left) and $|ER_{v,4}(x)|$ (right).

Figure 1 shows the curves of the error reminder functions $|ER_{u,4}(x)|$ and $|ER_{v,4}(x)|$ for $J = 4$. In Table 3, we have compared the maximal error remainders $MER_{u,5}$ and $MER_{v,5}$ obtained from the Haar wavelet method(HWM) for $J = 5$, along with the results obtained using the Chebyshev finite difference method [14] and the Adomian decomposition method, which is combined with the Duan-Rach modified recursion scheme [7].

Table 3. Comparison of the maximal error remainder parameters.

	HWM(J=5)	Ch.FD [14]	ADM [7]
$MER_{u,5}$	2.7991×10^{-6}	1.15556×10^{-6}	2.39928×10^{-4}
$MER_{v,5}$	8.2326×10^{-8}	3.39872×10^{-8}	7.05670×10^{-6}

Example 2. For the second problem, we select fixed parameters α_1, α_2, β_1, β_2 and κ, and apply the proposed Haar wavelet technique. As in the previous example, we define the error remainder functions to evaluate the

accuracy and efficiency of our approximate solutions:

$$ER_{u,J}(x) = u_J''(x) - \frac{\alpha_1 u_J(x) v_J(x)}{1 + \beta_1 u_J(x) + \beta_2 v_J(x)},$$
$$ER_{v,J}(x) = v_J''(x) - \frac{\alpha_2 u_J(x) v_J(x)}{1 + \beta_1 u_J(x) + \beta_2 v_J(x)}.$$

We set $\alpha_1 = 1,\ \alpha_2 = 2,\ \beta_1 = 1,\ \beta_2 = 3,\ \kappa = \frac{1}{2}$. In Tables 4 and 5, the obtained approximate solutions are compared to the results from the sinc-collocation method [22], the optimal homotopy analysis method [18] and Numerov's method(Nu-M) with a constant stepsize $h = 0.1$.

Table 4. Numerical solution for $u_3(x)$.

x	HWM($J = 3$)	OHAM [18]	Sinc-c [22]	Nu-M
0.1	0.9429110	0.9428972	0.9429145	0.9429102
0.3	0.8339846	0.8339414	0.8339840	0.8339829
0.5	0.7315479	0.7314845	0.7315460	0.7315460
0.7	0.6350107	0.6349490	0.6350083	0.6350092
0.9	0.5437943	0.5437652	0.5437939	0.5437938

Table 5. Numerical solution for $v_3(x)$.

x	HWM($J = 3$)	OHAM [18]	Sinc-c [22]	Nu-M
0.1	0.8417942	0.8415794	0.8419224	0.8422102
0.3	0.8559476	0.8557293	0.8560406	0.8562694
0.5	0.8830803	0.8828670	0.8831439	0.8833089
0.7	0.9220122	0.9218381	0.9220478	0.9221486
0.9	0.9715856	0.9715097	0.9715983	0.9716309

Also in Tables 6 and 7, we have compared $|ER_{u,6}(x)|$ and $|ER_{v,6}(x)|$ together with the some existing results in [8, 18, 21].

Now we change parameters and assign $\alpha_1 = 2,\ \alpha_2 = 3,\ \beta_1 = 1,\ \beta_2 = 3$ and $\kappa = 3$. In Tables 8 and 9, the absolute error remainders are shown for $J = 5$. In a different scenario, we consider $\alpha_1 = 1,\ \alpha_2 = 2,\ \beta_1 = 2,\ \beta_2 = 4$ and $\kappa = 2$. For $J = 6$, we apply the Haar wavelet method proposed in this work and calculate the error remainders (see Tables 10 and 11).

Table 6. Comparison of $|ER_{u,6}(x)|$ with some other methods,for $\alpha_1 = 1,\ \alpha_2 = 2,\ \beta_1 = 1,\ \beta_2 = 3,\ \kappa = \frac{1}{2}$.

x	HWM($J=6$)	ChFD [21]	OHAM [18]	ADM [8]
0	3.27×10^{-4}	6.51×10^{-4}	2.85×10^{-4}	6.42×10^{-4}
0.2	6.03×10^{-5}	1.04×10^{-4}	9.38×10^{-5}	3.21×10^{-5}
0.4	1.72×10^{-4}	1.07×10^{-4}	4.27×10^{-4}	5.85×10^{-4}
0.6	1.68×10^{-4}	1.00×10^{-4}	7.10×10^{-4}	1.23×10^{-3}
0.8	5.67×10^{-5}	8.51×10^{-5}	8.43×10^{-4}	1.74×10^{-3}

Table 7. Comparison of $|ER_{v,6}(x)|$ with some other methods,for $\alpha_1 = 1,\ \alpha_2 = 2,\ \beta_1 = 1,\ \beta_2 = 3,\ \kappa = \frac{1}{2}$.

x	HWM($J=6$)	ChFD [21]	OHAM [18]	ADM [8]
0	6.55×10^{-4}	1.30×10^{-3}	3.15×10^{-4}	6.31×10^{-4}
0.2	1.20×10^{-4}	2.08×10^{-4}	4.90×10^{-5}	9.80×10^{-5}
0.4	3.44×10^{-4}	2.14×10^{-4}	4.08×10^{-4}	8.17×10^{-4}
0.6	3.77×10^{-4}	2.00×10^{-4}	7.54×10^{-4}	1.50×10^{-3}
0.8	1.13×10^{-4}	1.70×10^{-4}	9.81×10^{-4}	1.96×10^{-3}

Table 8. Comparison of $|ER_{u,5}(x)|$ with some other methods, for $\alpha_1 = 2,\ \alpha_2 = 3,\ \beta_1 = 1,\ \beta_2 = 3$ and $\kappa = 3$.

x	HWM($J=5$)	ChFD [21]	OHAM [18]	ADM [8]
0	3.35×10^{-3}	1.11×10^{-2}	2.41×10^{-3}	8.19×10^{-4}
0.2	1.96×10^{-3}	1.81×10^{-3}	1.07×10^{-2}	1.24×10^{-2}
0.4	7.10×10^{-4}	1.92×10^{-3}	1.59×10^{-2}	1.87×10^{-2}
0.6	8.33×10^{-4}	1.85×10^{-3}	1.34×10^{-2}	1.30×10^{-2}
0.8	3.04×10^{-3}	1.62×10^{-3}	1.77×10^{-4}	9.28×10^{-3}

Table 9. Comparison of $|ER_{v,5}(x)|$ with some other methods, for $\alpha_1 = 2,\ \alpha_2 = 3,\ \beta_1 = 1,\ \beta_2 = 3$ and $\kappa = 3$.

x	HWM($J=5$)	ChFD [21]	OHAM [18]	ADM [8]
0	5.03×10^{-3}	1.66×10^{-2}	4.81×10^{-3}	7.22×10^{-3}
0.2	2.94×10^{-3}	2.72×10^{-3}	1.70×10^{-3}	2.55×10^{-3}
0.4	1.06×10^{-3}	2.89×10^{-3}	4.13×10^{-3}	6.20×10^{-3}
0.6	1.25×10^{-3}	2.78×10^{-3}	1.57×10^{-2}	2.36×10^{-2}
0.8	4.56×10^{-3}	2.43×10^{-3}	3.87×10^{-2}	5.80×10^{-2}

Table 10. Comparison of $|ER_{u,6}(x)|$ with some other methods, for $\alpha_1 = 1,\ \alpha_2 = 2,\ \beta_1 = 2,\ \beta_2 = 4, \kappa = 2$.

x	HWM($J=6$)	ChFD [21]	OHAM [18]	ADM [8]
0	3.25×10^{-4}	9.11×10^{-4}	3.44×10^{-5}	1.40×10^{-4}
0.2	6.39×10^{-5}	1.50×10^{-4}	1.31×10^{-4}	5.23×10^{-4}
0.4	1.97×10^{-4}	1.61×10^{-4}	3.88×10^{-4}	1.17×10^{-3}
0.6	2.10×10^{-4}	1.57×10^{-4}	4.16×10^{-4}	1.18×10^{-3}
0.8	7.73×10^{-5}	1.40×10^{-4}	1.11×10^{-4}	5.94×10^{-6}

Table 11. Comparison of $|ER_{v,6}(x)|$ with some other methods, for $\alpha_1 = 1,\ \alpha_2 = 2,\ \beta_1 = 2,\ \beta_2 = 4, \kappa = 2$.

x	HWM($J=6$)	ChFD [21]	OHAM [18]	ADM [8]
0	6.50×10^{-4}	1.82×10^{-3}	2.90×10^{-4}	5.80×10^{-4}
0.2	1.27×10^{-4}	3.01×10^{-4}	1.53×10^{-4}	3.06×10^{-4}
0.4	3.94×10^{-4}	3.23×10^{-4}	4.40×10^{-4}	8.80×10^{-4}
0.6	4.21×10^{-4}	3.15×10^{-4}	1.45×10^{-3}	2.90×10^{-3}
0.8	1.54×10^{-4}	2.80×10^{-4}	3.41×10^{-3}	6.83×10^{-3}

5 Conclusion

In this paper, we applied the Haar wavelet method to solve two systems of nonlinear differential equations that model two chemistry problems. The proposed technique transforms these systems into algebraic equations. The results indicate that the Haar wavelet method is a powerful tool for solving boundary value problems with a variety of boundary conditions. Also, this method is simple to apply, and the approximate solutions obtained using the Haar wavelet method show that this method is competitive with other numerical methods such as Adomian decomposition method [8], Sinc-collocation method [13,22], Chebyshev finite difference method [14,21], and optimal homotopy analysis method [18].

References

[1] B. Abbassi, S. Dullstein, N. Rabiger, Minimization of excess sludge production by increase of oxygen concentration in activated sludge ocs: experimental and theoretical approach, *Water Res.* **34** (2000) 139–146.

[2] M. Ahsan, W. Lei, A. A. Khan, A. Ullah, S. Ahmad, S. U. Arifeen, Z. Uddin, H. Qu, A high-order reliable and efficient Haar wavelet collocation method for nonlinear problems with two point-integral boundary conditions, *Alexandria Eng. J.* **71** (2023) 185–200.

[3] M. Ahsan, W. Lei, A. A. Khan, M. Ahmed, M. Alwuthaynani, A. Amjad, A higher-order collocation technique based on Haar wavelets for fourth-order nonlinear differential equations having nonlocal integral boundary conditions, *Alexandria Eng. J.* **86** (2024) 230–242.

[4] M. A. AL-Jawary, G. H. Radhi, The variational iteration method for calculating carbon dioxide absorbed into phenyl glycidyl ether, *IOSR J. Math.* **11** (2015) #99105.

[5] M. Asif, F. Bilal, R. Bilal, N. Haider, S. A. Abdelmohsenc, S. M. Eldind, An efficient algorithm for the numerical solution of telegraph interface model with discontinuous coefficients via Haar wavelets, *Alexandria Eng. J.* **72** (2023) 275–285.

[6] I. Aziz, S. Islam, M. Nisar, An efficient numerical algorithm based on Haar wavelet for solving a class of linear and nonlinear nonlocal boundary-value problems, *Calcolo.* **53** (2016) 621–633.

[7] J. S. Duan, R. Rach, A. M. Wazwaz, Oxygen and carbon substrate concentrations in microbial floc particles by the Adomian decomposition method, *MATCH Commun. Math. Comput. Chem.* **73** (2015) 785–796.

[8] J. S. Duan, R. Rach, A. M. Wazwaz, Steady-state concentrations of carbon dioxide absorbed into phenyl glycidyl ether solutions by the Adomian decomposition method, *J. Math. Chem.* **53** (2015) 1054–1067.

[9] S. Islam, I. Aziz, B. Sarler, The numerical solution of second-order boundary-value problems by collocation method with the Haar wavelets, *Math. Comput. Model.* **52** (2010) 1577–1590.

[10] J. Majak, B. S. Shvartsman, M. Kirs, M. Pohlak, H. Herranen, Convergence theorem for the Haar wavelet based discretization method, *Compos. Struct.* **126** (2015) 227–232.

[11] S. Muthukumar, M. Veeramuni, R. Lakshmanan, Analytical expression of concentration of substrate and oxygen in excess sludge production using Adomian decomposition method, *Indian J. Appl. Res.* **4** (2014) 387–391.

[12] S. Muthukaruppan, I. Krishnaperumal, R. Lakshmanan, Theoretical analysis of mass transfer with chemical reaction using absorption of carbon dioxide into phenyl glycidyl ether solution, *Appl. Math.* **3** (2012) 1179–1186.

[13] A. Saadatmandi, S. Fayyaz, Numerical study of oxygen and carbon substrate concentrations in excess sludge production using sinc-collocation method, *MATCH Commun. Math. Comput. Chem.* **80** (2018) 355–368.

[14] A. Saadatmandi, S. Fayyaz, Chebyshev finite difference method for solving a mathematical model arising in wastewater treatment plants, *Comput. Methods Diff. Eq.* **6** (2018) 448–455.

[15] K. Saranya, V. Mohan, L. Rajendran, Steady-state concentrations of carbon dioxide absorbed into phenyl glycidyl ether solutions by residual method, *J. Math. Chem.* **58** (2020) 1230–1246.

[16] R. Singh, V. Guleria, M. Singh, Haar wavelet quasilinearization method for numerical solution of Emden–Fowler type equations, *Math. Comput. Sim.* **174** (2020) 123–133.

[17] K. Singh, A. K. Verma, M. Singh, Higher order Emden–Fowler type equations via uniform Haar Wavelet resolution technique, *J. Comput. Appl. Math.* **376** (2020) #112836.

[18] R. Singh, A. M. Wazwaz, Steady-state concentrations of carbon dioxide absorbed into phenyl glycidyl ether: An optimal homotopy analysis method, *MATCH Commun. Math. Comput. Chem.* **81** (2019) 801–812.

[19] S. S. Tantawy, Solving linear systems of fractional integro-differential equations by Haar and Legendre wavelets techniques, *Partial Diff. Eq. Appl. Math.* **10** (2024) #100683.

[20] A. M. Wazwaz, R. Rach, J. S. Duan, Variational iteration method for solving oxygen and carbon substrate concentrations in microbial floc particles, *MATCH Commun. Math. Comput. Chem.* **76** (2016) 511–523.

[21] F. Zabihi, Chebyshev finite difference method for Steady-state concentrations of carbon dioxide absorbed into phenyl glycidyl ether, *MATCH Commun. Math. Comput. Chem.* **84** (2020) 131–140.

[22] F. Zabihi, The use of the sinc-collocation method for solving steady-state concentrations of carbon dioxide absorbed into phenyl glycidyl ether, *Comput. Methods Diff. Eq.* **12** (2024) 857–865.